Electronic Supplementary Information (ESI) for

Advanced asymmetric supercapacitors based on CNT@Ni(OH)$_2$ core-shell composites and 3D graphene networks

Huan Yi,[a] Huanwen Wang,[a] Yuting Jing,[a] Tianquan Peng,[a] Yiran Wang,[b]

Jiang Guo,[b] Qingliang He,[b] Zhanhu Guo*[b] and Xuefeng Wang*[a]

[a]*Department of Chemistry, and Shanghai Key Lab of Chemical Assessment and Sustainability, Tongji University，Shanghai 200092, China*

[b]*Integrated Composites Laboratory, Chemical & Biochemical Engineering, University of Tennessee; Knoxville, TN 37996, USA*

*Corresponding authors,

E-mail: xfwang@tongji.edu.cn (X. W);

zguo10@utk.edu (Z. G.).

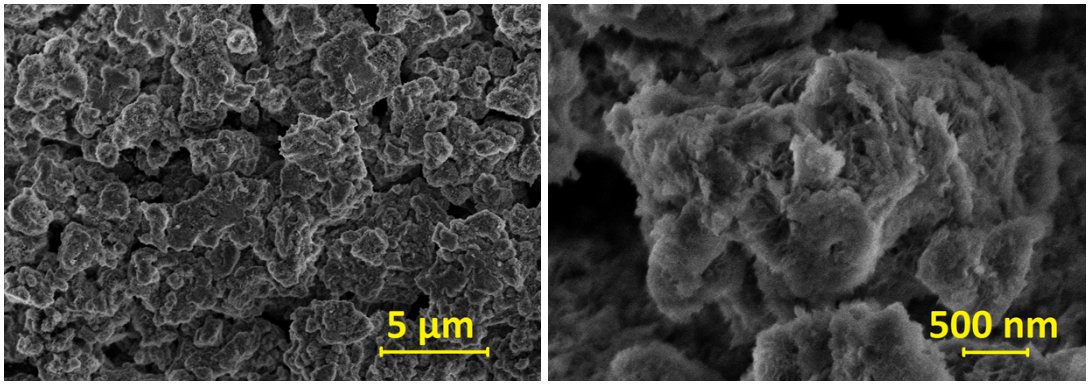

Fig. S1 FESEM images of the pure $Ni(OH)_2$.

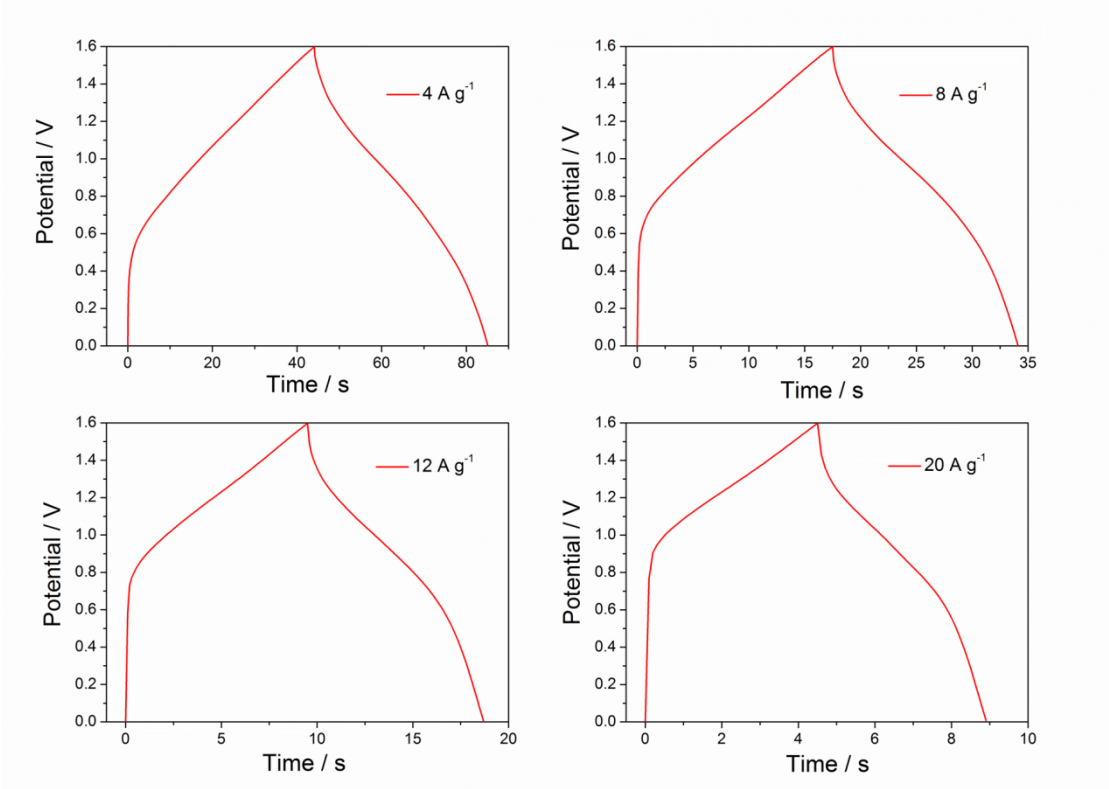

Fig. S2 GCD curves of CNT@$Ni(OH)_2$//3DGN ASC at various current densities.

The SEM images of CNT@$Ni(OH)_2$ before and after 200 cyclic voltammetry (CV) cycles are shown in Fig. S3. After 200 CV cycles, the overall core-shell structure of CNT@$Ni(OH)_2$ is well retained, while some slight aggregations happens and edges of $Ni(OH)_2$ nanosheets become somewhat blunt (Fig. S3 c,d), which can be attributed to the inevitable structure damage during the electrode preparation process and electrode activation. On the whole, the change of CNT@$Ni(OH)_2$ composite before and after 200 cycles is small, demonstrating the stability of this structure.

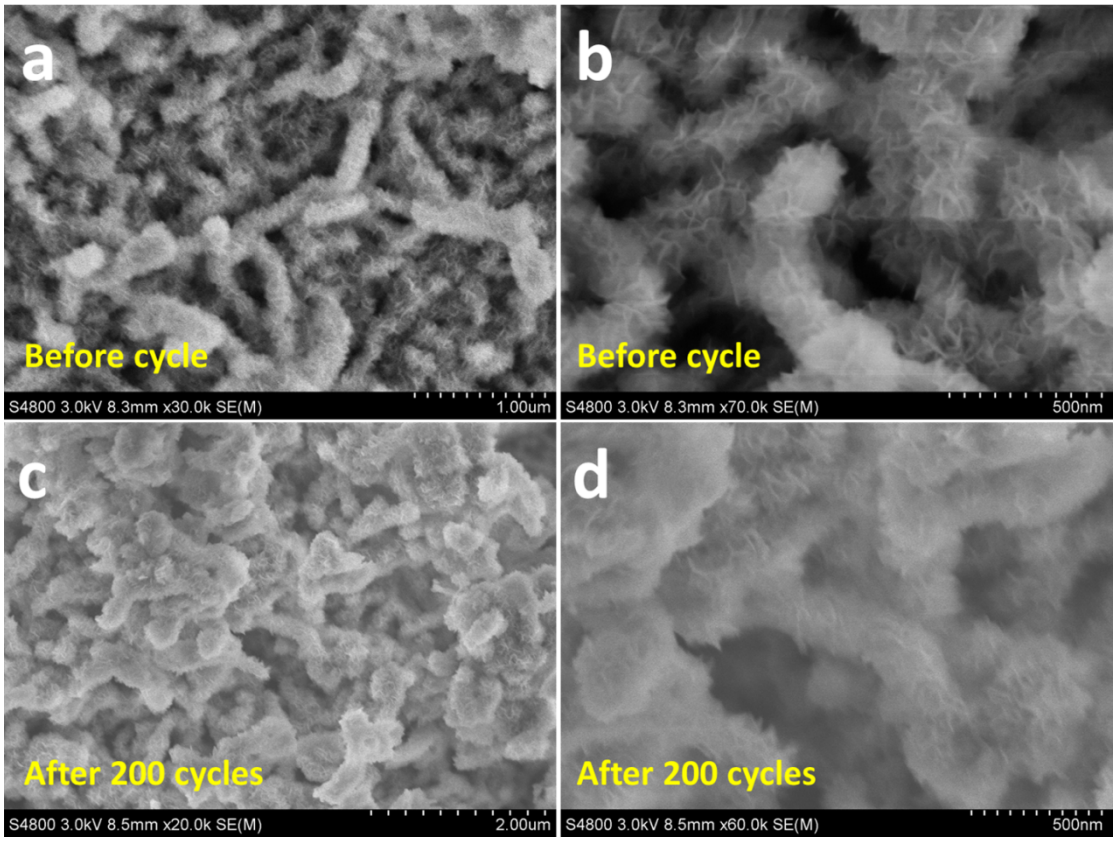

Fig. S3 SEM images of CNT@$Ni(OH)_2$ (a,b) before cycle and (c,d) after 200 CV cycles.

Table S1. Specific surface areas and pore parameters of 3DGN.

Sample	BET Surface Area ($m^2\ g^{-1}$)	Micropore Area ($m^2\ g^{-1}$)	Total Pore Volume ($cm^3\ g^{-1}$)	Micropore Volume ($cm^3\ g^{-1}$)	Average Pore Diameter (nm)
3DGN	134.7	11.2	0.33	0.004	6.6

Table S2. The specific capacitance, energy density and power density of the CNT@$Ni(OH)_2$//3DGN asymmetric supercapacitor calculated from the galvanostatic charge-discharge measurements.

Current density ($A\ g^{-1}$)	Discharge time (s)	Specific capacitance ($F\ g^{-1}$)	Energy density ($Wh\ kg^{-1}$)	Power density ($W\ kg^{-1}$)
1	197.9	123.68	43.98	800
2	92.6	115.75	41.16	1600
4	41.0	102.5	36.44	3200
8	16.6	83.0	29.51	6400
12	9.2	69.0	24.53	9600
20	4.4	55.0	19.56	16000

Note: the specific capacitance (C, $F\ g^{-1}$), Energy density (E, $Wh\ kg^{-1}$), and Power density (P, $W\ kg^{-1}$) are calculated from the discharge curve according to the following equation (1)-(3):

$$C = \frac{I \times t}{\Delta V \times m} \quad (1)$$

$$E = \frac{\frac{1}{2}CV^2}{3.6} \quad (2)$$

$$P = \frac{3600 \times E}{t} \quad (3)$$

Where I is the discharge current, t (s) is the discharge time, ΔV is the potential window, and m is the mass of the electrode.

Table S3. The energy and power densities of various asymmetric supercapacitors (ASCs) reported in literature.

ASCs	Energy density & power density	Loading mass (Total mass of two electrodes)	Current density (or scan rate)	Ref. (year)
MnO_2/carbon nanofiber composites//Activated carbon nanofibers	30.6 Wh kg^{-1} at 200 W kg^{-1}	Not reported	0.2 A g^{-1}	[46] (2013)
$Ni(OH)_2$//activated carbon	35.7 Wh kg^{-1} at 490 W kg^{-1}	0.94 mg cm^{-2}	5 mV s^{-1}	[47] (2013)
β-$Ni(OH)_2$/Ni-foam//activated carbon	36.2 Wh kg^{-1} at 100.6 W kg^{-1}	15.3 mg cm^{-2}	2 mA cm^{-2} (0.13 A g^{-1})	[48] (2014)
$NiCo_2O_4$-reduced graphite oxide//activated carbon	23.32 Wh kg^{-1} at 324.9 W kg^{-1}	4 mg cm^{-2}	0.5 A g^{-1}	[49] (2012)
Ni-Co oxide//activated carbon	7.4 Wh kg^{-1} at 1902.9 W kg^{-1}	6.3 mg cm^{-2}	20 mA cm^{-2} (3.17 A g^{-1})	[50] (2012)
MnO_2 nanowire/graphene//graphene	7.0 Wh kg^{-1} at 5000 W kg^{-1}	Not reported	5 A g^{-1}	[51] (2010)
$V_2O_5 \cdot 0.6H_2O$ nanoribbons//activated carbon	20.3 Wh kg^{-1} at 2000 W kg^{-1}	Not reported	2.22 A g^{-1}	[52] (2009)
CNT@$Ni(OH)_2$//3DGN	44.0 Wh kg^{-1} at 800 W kg_{-1} 19.6 Wh kg^{-1} at 16,000 W kg^{-1}	3.8 mg cm^{-2}	1 A g^{-1} 20 A g^{-1}	This work

References

[46] Wang, J.-G.; Yang, Y.; Huang, Z.-H.; Kang, F., A high-performance asymmetric supercapacitor based on carbon and carbon–MnO_2 nanofiber electrodes. *Carbon* **2013,** *61*, 190-199.

[47] Li, H. B.; Yu, M. H.; Wang, F. X.; Liu, P.; Liang, Y.; Xiao, J.; Wang, C. X.; Tong, Y. X.; Yang, G. W., Amorphous nickel hydroxide nanospheres with ultrahigh capacitance and energy density as electrochemical pseudocapacitor materials. *Nature communications* **2013,** *4*, 1894.

[48] Huang, J.; Xu, P.; Cao, D.; Zhou, X.; Yang, S.; Li, Y.; Wang, G., Asymmetric supercapacitors based on β-$Ni(OH)_2$ nanosheets and activated carbon with high energy density. *Journal of Power Sources* **2014,** *246*, 371-376.

[49] Wang, X.; Liu, W. S.; Lu, X.; Lee, P. S., Dodecyl sulfate-induced fast faradic process in nickel cobalt oxide–reduced graphite oxide composite material and its application for asymmetric supercapacitor device. *Journal of Materials Chemistry* **2012,** *22* (43), 23114.

[50] Tang, C.; Tang, Z.; Gong, H., Hierarchically Porous Ni-Co Oxide for High Reversibility Asymmetric Full-Cell Supercapacitors. *Journal of The Electrochemical Society* **2012,** *159* (5), A651.

[51] Wu, Z.-S.; Ren, W.; Wang, D.-W.; Li, F.; Liu, B.; Cheng, H.-M., High-Energy MnO_2 Nanowire/Graphene and Graphene Asymmetric Electrochemical Capacitors. *ACS Nano* **2010,** *4* (10), 5835-5842.

[52] Qu, Q. T.; Shi, Y.; Li, L. L.; Guo, W. L.; Wu, Y. P.; Zhang, H. P.; Guan, S. Y.; Holze, R., $V_2O_5 \cdot 0.6H_2O$ nanoribbons as cathode material for asymmetric supercapacitor in K_2SO_4 solution. *Electrochemistry Communications* **2009,** *11* (6), 1325-1328.

Table S4. The composition and preparation method of different materials.

	composition	preparation method [chemicals]
This work	Positive electrode: CNT@$Ni(OH)_2$ core-shell composite (α-$Ni(OH)_2$)	Chemical bath deposition (CBD) (80 °C, 2 h) [CNT, $Ni(NO_3)_2 \cdot 6H_2O$, urea, water]
	Negative electrode: 3D graphene network (graphene aerogel)	Hydrothermal + freeze-drying [graphene oxide, water]
Nano Research, 2013, **6**, 65-76	Graphene/$Ni(OH)_2$ hydrogel (β-$Ni(OH)_2$)	Hydrothermal (180 °C, 2 h) [graphene oxide, CNT, ammonia, hydrazine, $Ni(NO_3)_2$, water]
	Graphene-CNT/$Ni(OH)_2$ hydrogel (β-$Ni(OH)_2$)	
Adv. Funct. Mater., 2012, **22**, 1272-1278	$Ni(OH)_2$/CNT/Nickel foam (α-$Ni(OH)_2$)	Chemical vapor deposition (CVD) + CBD [aqueous ammonia, nickel sulfates, potassium persulfates, water]
RSC Adv., 2011, **1**, 484-489	CNT-doped $Ni(OH)_2$ nanosheets (α-$Ni(OH)_2$)	Hydrothermal (180 °C, 12 h) [CNT, N-methyl-pyrrolidone, $Ni(NO_3)_2 \cdot 6H_2O$, water]
Nano Energy, 2015, **11**, 211-218	CNT/$Ni(OH)_2$ composite (α- and β-$Ni(OH)_2$)	Chemical precipitation (60 °C, 20 min) [CNT, aqueous ammonia, nickel chloride, water]
Journal of Power Sources, 2013, **243**, 555-561	Reduced graphene oxide/CNT/α-$Ni(OH)_2$ composite (α-$Ni(OH)_2$)	Hydrothermal (120 °C, 24 h) [graphene oxide, CNT, $NiCl_2 \cdot 6H_2O$, urea, water]